




Cite this: *RSC Adv.*, 2019, 9, 450

Employing a novel O₃/H₂O₂ + BiPO₄/UV synergy technique to deal with thiourea-containing photovoltaic wastewater†

Zhikai Wei, Peng Li, Muhammad Hassan, Pu Wang, Cong Xu, Long-Fei Ren and Yiliang He *

Photovoltaic wastewater contains a large amount of thiourea that cannot be directly treated by biological methods because of its biotoxicity. In this study, a novel O₃/H₂O₂ + BiPO₄/UV synergy technique was used as a pre-treatment process to degrade thiourea. The effects of H₂O₂ and catalyst loading were investigated, and the transformation pathway of thiourea was predicted based on the intermediates detected by UPLC-Vion-IMS-QToF. The synergy technique degraded 89.14% thiourea within only 30 min, and complete degradation occurred after 150 min. The TOC removal of O₃/H₂O₂ + BiPO₄/UV was 1.8, 1.5, and 1.9 times that of O₃/H₂O₂ and BiPO₄/UV/H₂O₂ single processes and O₃/H₂O₂ + UV process, respectively, which was due to the synergy between H₂O₂ residues and BiPO₄. In addition, thiourea was mainly degraded by ·OH into thiourea dioxide and melamine (polymerized by other intermediates) and then further degraded into biuret and methyl carbamate by the holes of BiPO₄, followed by complete mineralization into H₂O and CO₂. These results confirm that the O₃/H₂O₂ + BiPO₄/UV synergy technique is a promising option for the degradation of thiourea.

Received 29th September 2018
 Accepted 23rd November 2018

DOI: 10.1039/c8ra08085b

rsc.li/rsc-advances

1. Introduction

Thiourea is widely used in numerous industries,^{1–4} especially in the photovoltaic industry. It is used in chemical bath deposition to produce CdS polycrystalline films for thin-film solar cells.⁵ Hence, wastewater from photovoltaic plants contains a large amount of redundant thiourea. It degrades slowly in the natural environment and has serious effects on human health.^{6–8} Due to the biological toxicity of thiourea,⁹ it cannot be treated directly by biological methods. Advanced oxidation processes (AOPs) can be an alternative method for the pre-treatment of photovoltaic wastewater containing high concentration of thiourea, transforming thiourea into other substances without biotoxicity.

Considering that photovoltaic wastewater contains high concentrations of organic matter and salts, the process we use cannot further introduce excess salt as it will be over-discharged. An O₃/H₂O₂ Fenton-like process was selected as it generates extraordinarily reactive hydroxyl radicals (·OH) by the reaction of ozone and hydrogen peroxide without salt introduction. These radicals subsequently attack and decompose contaminants in the water, and the process is usually effective,

simple, environment-friendly and economically sustainable. The O₃/H₂O₂ method enables rapid degradation of various recalcitrant organic compounds such as perfluorinated chemicals, dibutylsulfide, dimethyl sulfoxide, phenol and linear alkyl benzene.^{10–14} However, using H₂O₂ alone in the O₃/H₂O₂ process is not sufficient as excess H₂O₂ residues not only affect the degradation efficiency but also increase COD of the water sample and affect the post-treatment process.¹⁵

Some studies have improved the utilization efficiency of H₂O₂ residues by employing photo-irradiation.¹⁶ Nevertheless, ·OH generated by UV or O₃/H₂O₂ is inferior in organic mineralization as ·OH tends to abstract hydrogen from C–H bonds or add hydrogen to unsaturated carbon–sulfur bonds; if these bonds are not present (*e.g.*, oxalic acid, which is one of the intermediates in the degradation of phenol¹⁷), the oxidation ability of ·OH will be limited. A photocatalyst, namely, bismuth phosphate (BiPO₄) is considered an alternative as it can generate holes, which enhance the mineralization efficiency. It has been proven to be an efficient catalyst and has an optical indirect band gap of 3.85 eV. The photocatalytic activity of BiPO₄ is twice that of titanium dioxide (TiO₂ P25, Degussa).¹⁸ BiPO₄ possesses excellent photocatalytic activity due to the inductive effect of PO₄^{3–} since it can separate electrons and holes. BiPO₄ has been applied for the removal of dyes¹⁸ and phenols.¹⁹ BiPO₄ not only improves the mineralization efficiency but also has a synergistic effect with H₂O₂. In a previous study, BiPO₄ coupled with 60 mg L^{–1} H₂O₂ significantly improved the degradation efficiency of phenol²⁰. Adequate H₂O₂

School of Environmental Science and Engineering, Shanghai Jiao Tong University, 800 Dongchuan Road, 200240 Shanghai, PR China. E-mail: ylhe@sjtu.edu.cn; Tel: +86 21-54744008

† Electronic supplementary information (ESI) available. See DOI: 10.1039/c8ra08085b



interacted with BiPO_4 , improving the photocatalytic efficiency of BiPO_4 by increasing the separation efficiency of e^- and h^+ through the capture of e^- by H_2O_2 . Based on these facts, the $\text{O}_3/\text{H}_2\text{O}_2 + \text{BiPO}_4/\text{UV}$ synergy technique was developed in this study. We hypothesize that H_2O_2 residues after $\text{O}_3/\text{H}_2\text{O}_2$ treatment will be utilized by BiPO_4/UV , which is a novel approach.

In this study, we report the improvement in thiourea transformation efficiency and TOC removal by using the $\text{O}_3/\text{H}_2\text{O}_2 + \text{BiPO}_4/\text{UV}$ synergy technique coupled with the investigation of the utilization efficiency of residual H_2O_2 . We have also investigated the effects of H_2O_2 concentration and catalyst loading. The possible transformation pathway of thiourea is predicted in the end.

2. Material and methods

2.1 Solution preparation

Synthetic solutions were prepared using 18.2 M Ω cm Milli-Q deionized water. All the reagents used were of analytical grade. Thiourea was supplied by Aladdin (USA), ammonium chloride by Sinopharm Chemical reagent Co., Ltd. (China) and hydrogen peroxide (30% w/v) by Macklin (USA). For residual H_2O_2 test, potassium titanyl oxalate was purchased from Macklin (USA). Thiourea (1.2 g) and ammonium chloride (0.535 g) (as the source of ammonium nitrogen) were added into 1 L of deionized distilled water to simulate photovoltaic wastewater.

2.2 Preparation of BiPO_4

BiPO_4 nanorods were prepared *via* the reflux method.²¹ In short, 1.956 g of $\text{Bi}(\text{NO}_3)_3 \cdot 5\text{H}_2\text{O}$ (AR, Macklin) and 3.145 g of $\text{NaH}_2\text{PO}_4 \cdot 2\text{H}_2\text{O}$ (AR, Macklin) were added into a flask, followed by mixing with at least 750 mL of deionized water. After the pH was adjusted to 2.2 with concentrated nitric acid (Sinopharm Chemical reagent Co., Ltd.), the flask was placed in an oil bath

(120 °C) and mixing was conducted at 800 rpm, followed by heating for 48 hours. The resultant white precipitate was washed three times with deionized water and dried at 120 °C for 12 hours.

2.3 Experimental set-up and procedure

2.3.1 Experimental set-up. A self-designed experimental setup was employed in this study, as shown in Fig. 1. Ozone was generated using a laboratory ozone generator having a maximum generation capability of 32 g h^{-1} . The flow rate was adjusted to 5 L min^{-1} before inserting into the ozone reaction tower. The volume of the ozone reaction tower was 12 L. To fully mix the gas and liquid phases, a reflux unit was used in the ozone reaction tower with a reflux rate of 2 L min^{-1} . The reflux unit was equipped with a pH meter and a dosing pump to monitor the pH variation and H_2O_2 . After $\text{O}_3/\text{H}_2\text{O}_2$ treatment, samples were transferred into a photo reactor. The photo reactor included two low-pressure mercury lamps (254 nm, 11 W, Philips, China) housed inside a wooden box. The intensity of UV irradiation was 4.73 mW cm^{-2} , measured by an ultraviolet radiation meter (UV-C, photoelectric instrument factory of Beijing Normal University, China). The Petri factor for the low-pressure UV system was determined to be greater than 0.9.

2.3.2 Experimental procedure

$\text{O}_3/\text{H}_2\text{O}_2 + \text{BiPO}_4/\text{UV}$ synergy technique. $\text{O}_3/\text{H}_2\text{O}_2 + \text{BiPO}_4/\text{UV}$ synergy technique was carried out in the self-designed setup (Fig. 1). The optimum conditions for maximizing the TOC residues and specifying the hydrogen peroxide residues of $\text{O}_3/\text{H}_2\text{O}_2$ treatment were determined by means of a three-factor three-level Box–Behnken experimental design (BBD) combined with the response surface methodology (RSM) to correlate experimentally obtained criteria and experimental conditions given by the Box–Behnken experimental design. The independent variables were the initial concentrations of H_2O_2 (X_1) and

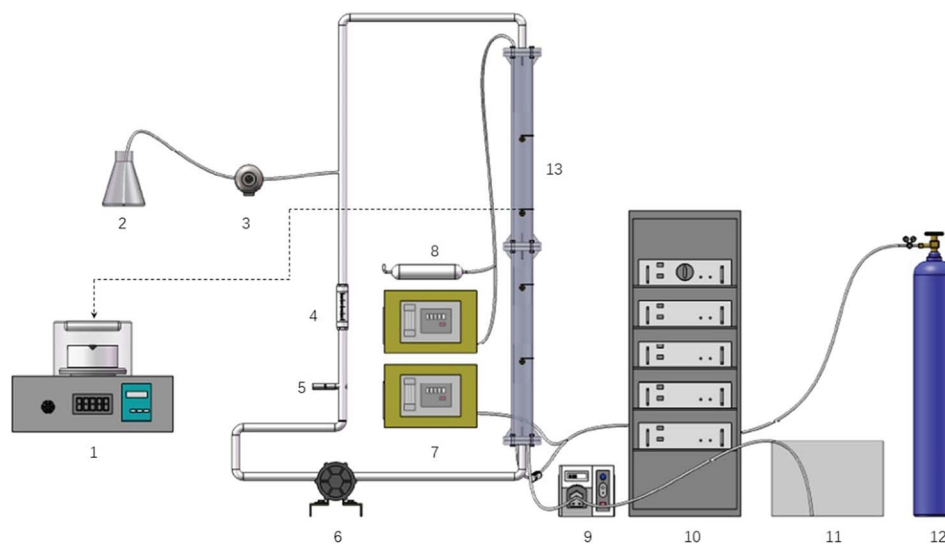


Fig. 1 Experiment reactor. (1): Photoreactor instrument; (2): agents can for H_2O_2 ; (3): agents pump; (4): flowmeter; (5): pH-meter; (6): circulating pump; (7): ozone meter; (8): ozone destructor; (9): peristaltic pump; (10): ozonator; (11): wastewater tank; (12): oxygen bottle; (13): reaction tower.



Table 1 Independent variables and their coded levels based on the Box–Behnken design

Independent variable	Symbol	Code levels		
		−1	0	1
H ₂ O ₂ (mL)	X ₁	10	45	80
O ₃ (mg L ^{−1})	X ₂	20	50	80
pH	X ₃	4	7	10

O₃ (X₂) and the initial pH (X₃), which were coded as −1, 0 and +1, as shown in Table 1.

The total number of experimental trials was 17 based on a three level and a three factor experimental design with three replicates at the centre of the design to estimate a pure error sum of squares. TOC residues, H₂O₂ residues and the 'pseudo'-second order rate constant were considered as dependent factors (process responses). Specific experimental conditions of the O₃/H₂O₂ treatment were selected according to the reaction model generated by BBD. The experimental conditions could achieve the desired reaction results of the O₃/H₂O₂ treatment process. After 150 min of the O₃/H₂O₂ treatment, the treated effluent (100 mL) was transferred into a low-pressure (LP) UV collimated beam system with a specific amount of BiPO₄ after stirring and ultrasonication for 10 min before irradiation. The UV intensity was 4.73 mW cm^{−2} in average and the BiPO₄/UV post-treatment lasted for 180 minutes.

O₃/H₂O₂ + UV process. The experimental procedure of the O₃/H₂O₂ + UV process was similar to that of the O₃/H₂O₂ + BiPO₄/UV synergy technique. Experimental conditions of the O₃/H₂O₂ treatment were also selected according to the reaction model generated by BBD. The conditions were the same as that of the O₃/H₂O₂ + BiPO₄/UV synergy technique to compare their mineralization efficiencies. However, BiPO₄ was not added in the post-treatment process. Samples were directly transferred into the LP UV collimated beam system.

O₃/H₂O₂ single-process. The initial experimental conditions and the procedures of the O₃/H₂O₂ single-process were the same as those of the O₃/H₂O₂ + BiPO₄/UV synergy technique; however, there was no post-treatment in this process. The O₃/H₂O₂ treatment was sustained for 330 minutes.

BiPO₄/UV/H₂O₂ process. BiPO₄/UV/H₂O₂ process was carried out in the LP UV collimated beam system in the same manner as before. The initial amounts of H₂O₂ and BiPO₄ loadings were equal to those used in the O₃/H₂O₂ + BiPO₄/UV synergy technique. A specific amount of BiPO₄ was added after agitation and ultrasonication for 10 min before irradiation. The experiment was continued for 330 minutes.

A water sample (3 mL) was taken every 30 minutes from the reactor in each experiment mentioned above to analyse the TOC concentration and H₂O₂ residues. Moreover, three replicates were made for each analytical measurement.

2.4 Analytical methods

The concentration of thiourea was analyzed by a HPLC system (Agilent 6120B, USA) equipped with a multi-wavelength UV

detector (ESI, Text S1†). TOC was monitored with a Multi N/C 3100 TOC/TN analyzer. H₂O₂ was measured by a spectrophotometric method²² using a HACH DR6000 UV-vis spectrophotometer. Ammonium nitrogen was determined by salicylic acid spectrophotometry (HJ 536-2009 in China). Nitrate nitrogen, sulfate and chloridion were determined by ion chromatography (Metrohm 820 IC). The morphology and the structure of the BiPO₄ photocatalyst were examined with a scanning electron microscope (SEM) and powder X-ray diffraction (XRD). The Brunauer Emmett Teller (BET) specific surface area and the pore size distribution of the BiPO₄ photocatalyst were characterized by nitrogen adsorption at 77 K with Micromeritics 3020. The degradation by-products of thiourea were analysed *via* high resolution mass spectrometry analysis carried out on Water I-Class Acquity UPLC (Waters, UK) coupled with Vion IMS QToF (Waters, UK) (ESI, Text S2†).

3. Results and discussion

3.1 Experimental design and condition selection

The Box–Behnken statistical experiment design was employed to investigate the effects of three independent variables on the TOC and H₂O₂ residues as response functions. Table 2 depicts the three-factor three-level Box–Behnken experimental design and the observed and predicted values for the TOC and H₂O₂ residues by the developed quadratic model.

As mentioned before, RSM was used to estimate the parameters, indicating an empirical relationship between the input variables and the response, as shown in eqn (1) and (2). The quadratic model equation for predicting the response function (TOC, H₂O₂ residues) could be expressed by the following second-order polynomial equation in terms of the coded factors:

Table 2 Three-factor three-level BBD for RSM along with the observed and predicted responses

Run	Independent code variables			TOC		H ₂ O ₂	
	H ₂ O ₂	O ₃	pH	Observed	Predicted	Observed	Predicted
1	1	0	−1	173.4	173.4	1046.9	1053
2	−1	−1	0	179.2	177.4	2.22	0.86
3	−1	0	−1	175	176.9	9.93	0.86
4	0	0	0	175.6	168.2	442.27	416.51
5	0	−1	1	172.8	174.4	316.08	329.84
6	1	1	0	160.2	161.8	855.02	862.77
7	0	0	0	168.8	168.2	415.98	416.51
8	0	1	−1	175.6	174	350.26	336.5
9	0	−1	−1	175	174.7	389.69	410.97
10	−1	0	1	182.4	182.2	0.86	0.86
11	0	1	1	167.6	167.9	242.47	221.18
12	0	0	0	166.2	168.2	405.46	416.51
13	0	0	0	164.8	168.2	392.32	416.51
14	1	0	1	163.4	161.6	844.51	858.04
15	1	−1	0	157	157.3	1120.6	1093.3
16	0	0	0	165.4	168.2	426.5	416.51
17	−1	1	0	166	165.8	14.53	41.82



$$Y = 168.16 - 6.07X_1 - 1.82X_2 - 1.60X_3 + 4.10X_1X_2 - 4.35X_1X_3 - 1.45X_2X_3 - 0.88X_1^2 - 1.68X_2^2 + 6.27X_3^2 \quad (1)$$

$$Z = 416.51 + 479.94X_1 - 45.78X_2 - 49.11X_3 - 69.46X_1X_2 - 48.34X_1X_3 - 8.54X_2X_3 + 116.26X_1^2 - 34.68X_2^2 - 57.20X_3^2 \quad (2)$$

Here, Y and Z are the predicted responses for TOC and H_2O_2 residues, and X_1 , X_2 and X_3 are the independent variables.

The statistical significance of the second-order polynomial model to predict the TOC and H_2O_2 residues was tested by the analysis of variance (ANOVA). The results of ANOVA are presented in Table S1 and Table S2 (ESI, Table S1 and S2†). The significance of each coefficient in eqn (1) and (2) was determined by the Fisher's F -test and the values of probability were greater than F .

A small probability value ($p < 0.0001$) indicated that the model was highly significant. The goodness of fit of the model was validated by the determination coefficient (R^2). In this case, R^2 values were 0.99758 and 0.874188, which showed high significance of the model. Also, the adequate precision greater than 4 (54.69 and 8.84 in this case) showed that the model could be used to navigate the design space defined by BBD. Adequate precision is a measure of the range in the predicted response relative to its associated error. The normality of data can be checked through the high correlation between observed and predicted data shown in Fig. S3 (ESI, Fig. S3†), which indicates their low discrepancies.

To study the interaction effects between the variables (initial concentration of polymer, initial concentration of H_2O_2 , pH and recirculation rate), the 3D response surface and 2D contour curves based on the quadratic model were plotted, as shown in Fig. 2(a–f).

As illustrated in Fig. 2(a–f), TOC was significantly affected by the initial H_2O_2 dosage and O_3 concentration. It can be seen that TOC decreased with increasing H_2O_2 dosage and O_3 concentration. The effects of the initial H_2O_2 dosage and the O_3 concentration are mainly due to the generation of $\cdot OH$ by H_2O_2 and O_3 . The more the $\cdot OH$, the higher the mineralization efficiency. Also, it can be seen that minimum TOC is achieved at pH of 7. In alkaline solutions, the dissociated form of hydrogen peroxide (HO_2^-) reacts with $\cdot OH$ more than 2 orders of magnitude faster than hydrogen peroxide.²³ Therefore, the oxidation efficiency decreases as $\cdot OH$ species are consumed. However, in acidic solutions, thiourea is stable and relatively hard to be mineralized. As for the amount of H_2O_2 residues, data are illustrated from Fig. 2(d)–(f). The initial H_2O_2 dosage is the main factor that influences the amount of H_2O_2 residues; however, the influence of pH and O_3 concentration is much less pronounced than that of the initial H_2O_2 dosage. This is also confirmed in Table S2,† which shows the significance of the factors and their interaction.

To investigate the mineralization and degradation efficiency of the $O_3/H_2O_2 + BiPO_4/UV$ synergy technique, we chose the initial experimental conditions of O_3/H_2O_2 treatment based on the quadratic model equation calculated by BBD. According to these equations, specific experimental conditions were selected

to achieve the maximum mineralization efficiency of thiourea under a targeted amount of H_2O_2 residues. In this experiment, we set the experimental conditions to obtain $70 \text{ mg L}^{-1} H_2O_2$ residues from the O_3/H_2O_2 treatment with the maximum mineralization efficiency. According to this target, the ozone concentration was set at 55.71 mg L^{-1} , the initial concentration of H_2O_2 was 435 mg L^{-1} , and the initial pH value was 9.20.

3.2 Comparison of mineralization efficiencies among different treatment processes

In this study, degradation efficiencies were compared among different treatment processes. As observed in Fig. 3, 89.14% of thiourea was degraded by O_3/H_2O_2 within only 30 minutes. The chemical construction of thiourea includes a double bond between carbon and sulfur. It can be easily oxidized by an oxidizing agent, especially by strong oxidants such as ozone ($E^0 = 2.07 \text{ eV}$), hydrogen peroxide ($E^0 = 1.28 \text{ eV}$) and hydroxyl radicals ($E^0 = 2.8 \text{ eV}$). The $\cdot OH$ species generated by O_3/H_2O_2 as well as O_3 and H_2O_2 oxidize thiourea into other products, which may contribute to the degradation of thiourea. The degradation efficiency of thiourea by UV/H_2O_2 and $BiPO_4/UV/H_2O_2$ processes was also investigated and compared with that of O_3/H_2O_2 . In only 30 minutes of reaction time, 69.35% and 71.90% of thiourea were degraded by UV/H_2O_2 and $BiPO_4/UV/H_2O_2$, respectively, which were much lower than the value obtained for O_3/H_2O_2 . The lower degradation efficiency might be due to the absence of O_3 in the process, which reduced their oxidizability.

The O_3/H_2O_2 process only reduced 23.125 mg L^{-1} TOC, whereas $O_3/H_2O_2 + UV$ achieved TOC reduction of 22.5 mg L^{-1} ; also, the performance of the $BiPO_4/UV/H_2O_2$ single-process was much lower than that of the $O_3/H_2O_2 + BiPO_4/UV$ synergy technique. Nevertheless, Fig. 3 shows that the O_3/H_2O_2 single-process achieved more TOC removal in the first half of the treatment process than the $BiPO_4/UV/H_2O_2$ single-process; however, in the second half, the TOC removal rate of the O_3/H_2O_2 single-process was exceeded by that of the $BiPO_4/UV/H_2O_2$ single-process. Based on this phenomenon, the $O_3/H_2O_2 + BiPO_4/UV$ synergy technique was applied to exert higher TOC removal and generate synergy effect. The amount of TOC removal by the $O_3/H_2O_2 + BiPO_4/UV$ synergy technique was 1.8 and 1.5 times higher than that of the O_3/H_2O_2 single-process and the $BiPO_4/UV/H_2O_2$ single-process, respectively. Also, the TOC removal was much higher than that without $BiPO_4$ addition, which was 1.9 times that of the $O_3/H_2O_2 + UV$ process. This is mainly due to two factors. The first factor is the synergy between $BiPO_4$ and H_2O_2 residues from O_3/H_2O_2 . The H_2O_2 residues from O_3/H_2O_2 are not wasted, and they further generate $\cdot OH$ through UV irradiation; H_2O_2 residues can also capture e^- generated in $BiPO_4$, which can increase the separation efficiency of e^- and h^+ .²⁰ Also, a part of H_2O_2 is utilized in O_3/H_2O_2 ; thus, we can avoid the negative effect on the synergy between $BiPO_4$ and H_2O_2 due to excess H_2O_2 . In $BiPO_4/UV/H_2O_2$ single-process, excess H_2O_2 shows inhibition of the synergy between $BiPO_4$ and H_2O_2 ; it can occupy the holes in $BiPO_4$ but cannot improve the separation efficiency of e^- and h^+ . Thus, the TOC removal of the $BiPO_4/UV/H_2O_2$ single-process is limited.



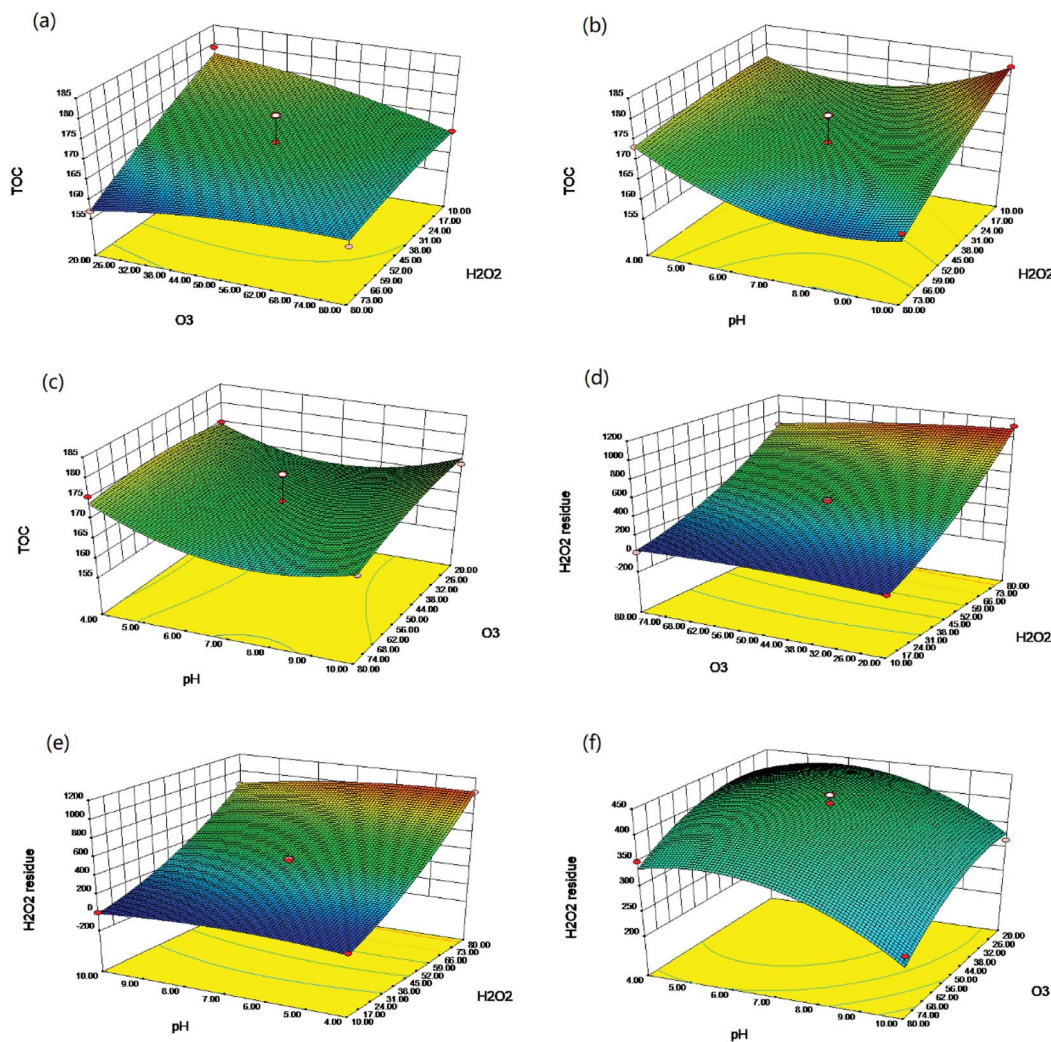


Fig. 2 Interaction effects of different parameters on TOC (a–c) and H₂O₂ residues (d–f) using 3D response surface and 2D contours: (a) O₃ concentration and initial H₂O₂ dosage, (b) pH and H₂O₂ dosage, (c) pH and O₃ concentration, (d) O₃ concentration and H₂O₂ dosage, (e) pH and H₂O₂ dosage, (f) pH and O₃ concentration.

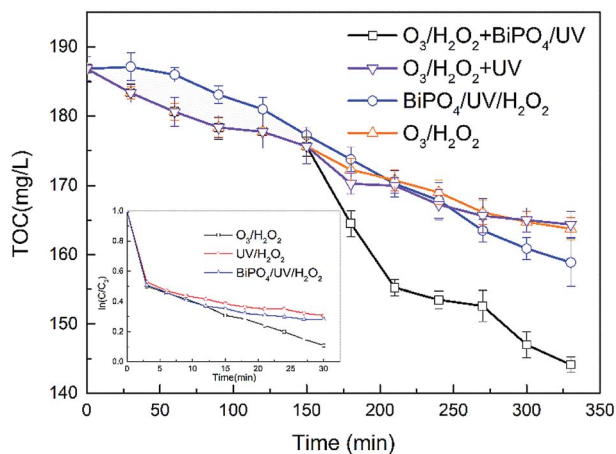


Fig. 3 Comparison of mineralization efficiencies among O₃/H₂O₂ + BiPO₄/UV synergy technique, O₃/H₂O₂ + UV, O₃/H₂O₂ and BiPO₄/UV/H₂O₂ processes and the degradation efficiencies among O₃/H₂O₂, UV/H₂O₂ and BiPO₄/UV/H₂O₂.

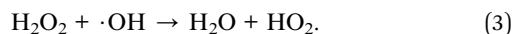
The second factor is the electron transfer oxidation of holes. ·OH tends to abstract hydrogen from C–H bonds or add hydrogen to unsaturated carbon–sulfur bonds; thus, it is superior in thiourea degradation but inferior in further mineralization. As for O₃/H₂O₂, it can only generate ·OH that is inferior in mineralization; thus, the amount of TOC removal is much lower than that of the processes containing BiPO₄. In contrast, BiPO₄ in BiPO₄/UV can generate holes that can directly mineralize the by-products of O₃/H₂O₂.

3.3 Comparison of H₂O₂ utilization among different treatment processes

The O₃/H₂O₂ + BiPO₄/UV synergy technique could greatly improve the utilization efficiency of hydrogen peroxide, especially in the BiPO₄/UV process, as shown in Fig. 4. After the treatment of O₃/H₂O₂, about 70 mg L⁻¹ hydrogen peroxide was retained, which could be utilized by BiPO₄ photocatalysis in less than 1 h. The O₃/H₂O₂ single-process and O₃/H₂O₂ + UV needed



more than 2 and 3 hours to consume hydrogen peroxide residues. Even though the consumption rate of hydrogen peroxide was higher in the BiPO₄/UV/H₂O₂ single-process, the TOC removal rate of thiourea was 15%, as mentioned before, which was much lower than that of the O₃/H₂O₂ + BiPO₄/UV synergy technique. It has been proven that hydroxide radicals are quenched by additional hydrogen peroxide species;^{24,25} thus, the hydroxide radicals generated in BiPO₄/UV/H₂O₂ single-process were not attached to thiourea but were consumed by extra H₂O₂ according to equation:²⁶



Therefore, excess H₂O₂ could lead to the consumption of active oxidizing hydroxyl radicals by a reaction other than the thiourea mineralization reaction, consequently reducing the rate of the latter reaction and wasting considerable H₂O₂ reagent.

In the O₃/H₂O₂ + BiPO₄/UV synergy technique, it is believed that H₂O₂ generates more ·OH in BiPO₄/UV because of the synergy between BiPO₄ and H₂O₂. Electron spin resonance (ESR) was carried out to investigate the hydroxyl radicals generated by H₂O₂, BiPO₄ or both BiPO₄ and H₂O₂ under UV irradiation. We measured hydroxyl radicals by ESR using DMPO as the spin-trap reagent. As shown in Fig. 5, the characteristic four peaks of DMPO·OH with the intensities of 1 : 2 : 2 : 1 appeared in all spectra. The intensity of ·OH generated in BiPO₄ after the addition of 70 mg L⁻¹ hydrogen peroxide was much higher than that in the H₂O₂ system and BiPO₄ system. The result was in accordance with that of Elmolla's research.²⁷ As an electron scavenger, H₂O₂ can react with e⁻, as shown in the following equation:

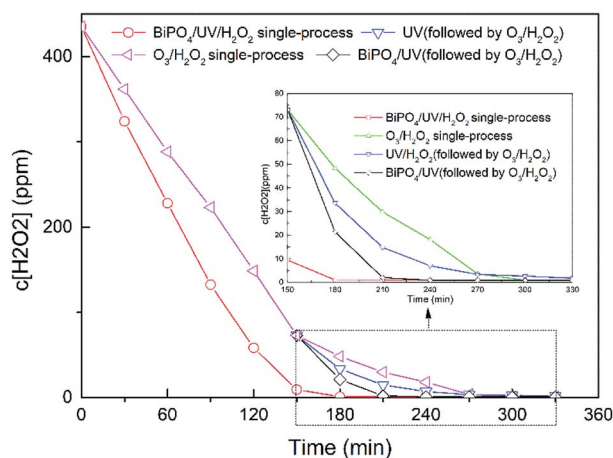
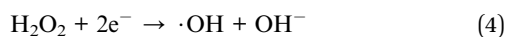


Fig. 4 Comparison of H₂O₂ utilization in different processes. The concentration of thiourea was 1.2 g L⁻¹, the concentration of ammonia nitrogen was 140 mg L⁻¹, the initial concentration of H₂O₂ was 435 mg L⁻¹, O₃ concentration was 55.71 mg L⁻¹, UV intensity was 4.73 mW cm⁻², and the BiPO₄ loading was 0.5 g L⁻¹.

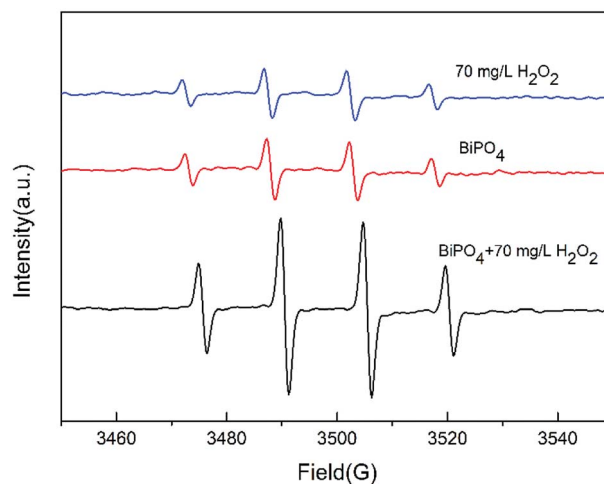


Fig. 5 DMPO spin-trapping ESR spectra under UV irradiation for 2 min at room temperature water in the presence of BiPO₄, H₂O₂ or both BiPO₄ and H₂O₂.

As explained before, an appropriate amount of H₂O₂ will capture the electrons in BiPO₄, increasing the separation efficiency of e⁻ and h⁺. This reaction also motivates H₂O₂ to generate ·OH. As a result, the electron capture process combined with the UV irradiation process increases ·OH generation; thus, it accelerates the consumption rate of residual H₂O₂ from O₃/H₂O₂ treatment. Also, more ·OH generation indicates less residual H₂O₂, and it will change the ratio of ·OH and H₂O₂; thus, ·OH scavenger reaction will be limited and H₂O₂ will be used efficiently. Nonetheless, the residual H₂O₂ from O₃/H₂O₂ not only increases the separation of e⁻ and h⁺ in BiPO₄, but also results in ·OH generation. Thus, high degradation of thiourea by O₃/H₂O₂ and residual H₂O₂ is efficiently utilized by the synergy between H₂O₂ and BiPO₄, attaining faster H₂O₂ consumption and higher TOC removal.

3.4 Effect of hydrogen peroxide

To investigate the effect of H₂O₂, different concentrations of H₂O₂ were employed in the O₃/H₂O₂ + BiPO₄/UV synergy technique. Based on the BBD model introduced before, we could predict the amount of residual H₂O₂ of O₃/H₂O₂ under different H₂O₂ concentrations. We set 70 mg L⁻¹, 140 mg L⁻¹ and 280 mg L⁻¹ as target H₂O₂ residues; 17.34 mL, 22.09 mL and 47.63 mL H₂O₂ were selected as initial concentrations.

Table 3 shows various experimental parameters. Under these treatment conditions, we compared the TOC removal rates between BiPO₄/UV and UV after the treatment of O₃/H₂O₂. Fig. 6(a) shows that BiPO₄ can significantly improve TOC removal under about 70 mg L⁻¹ residual H₂O₂. The TOC removal was 2.8 times that of the treatment without BiPO₄ addition. However, along with the increase in residual H₂O₂, the mineralization ability of BiPO₄/UV was inhibited. We can see from Fig. 6(b) and (c) that the mineralization efficiency of BiPO₄/UV was lower than that of the treatment without the BiPO₄ addition in the initial 60 and 90 minutes. This phenomenon can be explained by the following equation:²⁸



Table 3 Different experimental parameters for the O₃/H₂O₂ treatment

Run	Independent code variables			TOC		H ₂ O ₂	
	H ₂ O ₂ (mL)	O ₃ (mg L ⁻¹)	pH	Observed	Predicted	Observed	Predicted
1	17.3	57.71	9.2	175.63	178	74.47	70
2	22.1	62.88	7.5	174.75	172	138.10	140
3	47.6	77.10	9.7	167.75	169	239.53	280



$$-\ln\left(\frac{c[\text{H}_2\text{O}_2]_t}{c[\text{H}_2\text{O}_2]_0}\right)_{\text{average}} = k_0 t + c \quad (6)$$

Excess H₂O₂ might be absorbed on the surface of the BiPO₄ photocatalyst and can react with the holes on the surface of the catalyst. Since holes govern the mineralization efficiency of thiourea, consumption of holes by the absorbed H₂O₂ can result in retarded photocatalytic mineralization efficiency of thiourea. Also, excessive H₂O₂ can counteract the synergy between H₂O₂ residues and BiPO₄ photocatalyst. Excessive H₂O₂ may scavenge the holes as well as ·OH generated by e⁻ and H₂O₂. Thus, adequate H₂O₂ can improve the synergy between residual H₂O₂ and BiPO₄, but superfluous H₂O₂ may cause negative effects and lead to the decline in the mineralization efficiency of the O₃/H₂O₂ + BiPO₄/UV synergy technique.

As shown in Fig. 7, we also investigated the residual H₂O₂ consumption rate by BiPO₄/UV under conditions described in Table 3. The consumption rate of residual H₂O₂ by UV was calculated under 70 mg L⁻¹, 140 mg L⁻¹ and 280 mg L⁻¹ H₂O₂ concentrations, which conformed to pseudo first order reaction kinetics (eqn (6)):

Here, *k*₀ is the reaction kinetic constant, *c* is the intercept, *c*[H₂O₂]_{*t*} is the H₂O₂ concentration after reaction for different periods, and *c*[H₂O₂]₀ is the initial H₂O₂ concentration. The residual H₂O₂ consumption rates by the BiPO₄/UV system with different H₂O₂ concentrations were fit to eqn (7):

$$-\ln\left(\frac{c[\text{H}_2\text{O}_2]_t}{c[\text{H}_2\text{O}_2]_0}\right) = k_p t^2 + k_j t + c \quad (7)$$

Here, *k*_p and *k*_j are the coefficients of the BiPO₄/UV system with different H₂O₂ residues, *c* is the intercept, *c*[H₂O₂]_{*t*} is the H₂O₂ concentration after reaction for different periods, and *c*[H₂O₂]₀ is the initial H₂O₂ concentration.

As shown in Fig. 7, BiPO₄ can accelerate H₂O₂ consumption under 70 mg L⁻¹ of residual H₂O₂. Nevertheless, along with the increase in residual H₂O₂ to 140 mg L⁻¹ and 280 mg L⁻¹, BiPO₄ inhibited H₂O₂ consumption at the beginning; however, after

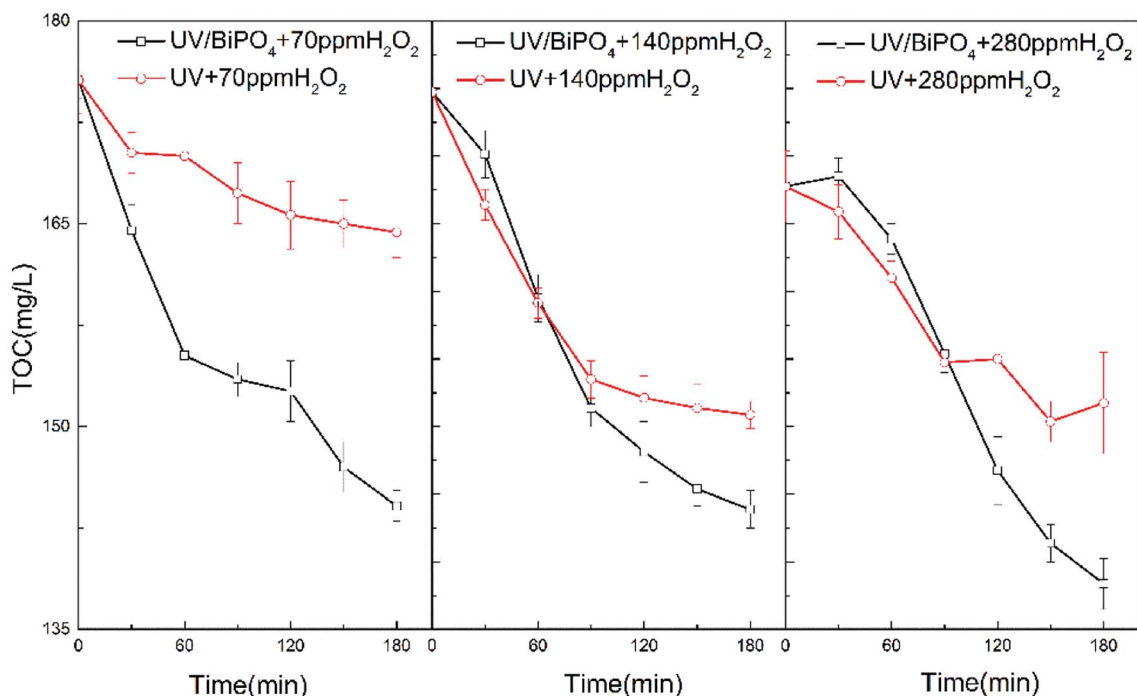


Fig. 6 Effect of different H₂O₂ residues of the H₂O₂/O₃ pre-treatment on the TOC removal: parameters carried out according to Run 2 with 74.47 mg L⁻¹ H₂O₂ residues, Run 3 with 138.10 mg L⁻¹ H₂O₂ residues and Run 3 with 239.53 mg L⁻¹ H₂O₂ residues.



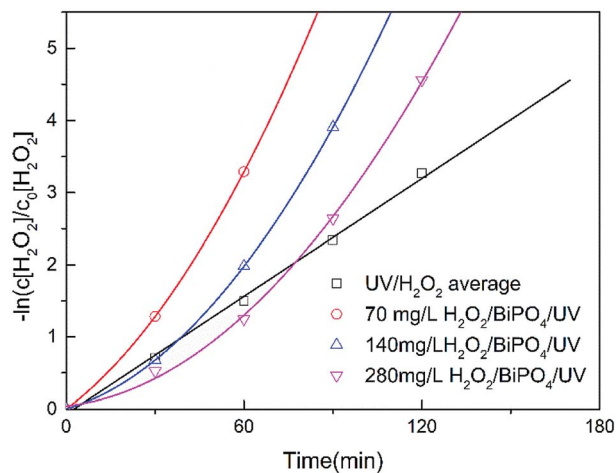


Fig. 7 The consumption rate of H_2O_2 under UV and BiPO_4/UV with about 70, 140, 280 mg L^{-1} H_2O_2 residues.

the residual H_2O_2 was partially consumed, the consumption rate was expedited and exceeded the rate of the UV system. This phenomenon shows inactivation of H_2O_2 in the BiPO_4/UV system under high concentrations of H_2O_2 residues because UV irradiation is first absorbed by the BiPO_4 photocatalyst. Under this circumstance, less H_2O_2 can be driven to generate $\cdot\text{OH}$, and the consumption amount of H_2O_2 decreases. Although, e^- and h^+ on the surface of BiPO_4 can consume H_2O_2 as explained before, considering that the amount of the BiPO_4 photocatalyst is constant under these three conditions, the consumption amount of H_2O_2 does not change. Thus, the consumption rate of H_2O_2 in BiPO_4/UV post-treatment decreases along with the increase in H_2O_2 concentration. This influences the TOC removal rate of the $\text{O}_3/\text{H}_2\text{O}_2 + \text{BiPO}_4/\text{UV}$ synergy technique and also the utilization efficiency of the H_2O_2 reagent.

3.5 Effect of photocatalyst loading

The amount of BiPO_4 is another important parameter in the $\text{O}_3/\text{H}_2\text{O}_2 + \text{BiPO}_4/\text{UV}$ synergy technique. To investigate the effect of BiPO_4 loading on the TOC removal of thiourea by the $\text{O}_3/\text{H}_2\text{O}_2 + \text{BiPO}_4/\text{UV}$ synergy technique, 0.2 g L^{-1} , 0.5 g L^{-1} , 1.0 g L^{-1} and 1.5 g L^{-1} of BiPO_4 were loaded in the post-treatment process. We used TOC removal to show the treatment effect and used the ratio between the TOC removal and the BiPO_4 loading to show the catalyst efficiency. As shown in Fig. 8, when the amount of BiPO_4 was increased from 0.2 g L^{-1} to 0.5 g L^{-1} , the TOC removal improved from 6.125 mg L^{-1} to 30.875 mg L^{-1} and the catalyst efficiency was greatly enhanced. However, upon further increasing the BiPO_4 loading to 1.0 g L^{-1} and 1.5 g L^{-1} , neither the TOC removal nor the catalyst efficiency decreased significantly, revealing negative effect on thiourea mineralization. This phenomenon showed a similar tendency to that reported in other researches:^{29,30} the mineralization efficiency cannot always increase with the increase in catalyst loading. Many studies have shown that the mineralization efficiency of a photocatalyst is strongly affected by the number of active sites and the photoabsorption ability of the catalyst used.³¹ Adequate

catalyst loading increases the generation rate of e^-/h^+ pairs; hence, we observe the formation of $\cdot\text{OH}$ for enhancing photo-degradation and the formation of holes for enhancing mineralization. However, an excess dosage of the catalyst decreases light penetration *via* the shielding effect of suspended particles^{32,33} and thereby reduces the degradation and mineralization rates. Although the $\text{O}_3/\text{H}_2\text{O}_2 + \text{BiPO}_4/\text{UV}$ synergy technique exhibits a synergistic effect between H_2O_2 and BiPO_4 , it still cannot avoid the shielding effect. Excess BiPO_4 reduces the incident light intensity by reflection despite the large number of active sites present.

3.6 Mineralization mechanism of thiourea

To elucidate the degradation pathways of thiourea by the $\text{O}_3/\text{H}_2\text{O}_2 + \text{BiPO}_4/\text{UV}$ synergy technique, the reaction intermediates were detected by UPLC-IM-QTOF-MS (ESI, Fig. S4†); four compounds were identified with peaks of m/z 107 and m/z 126 after $\text{O}_3/\text{H}_2\text{O}_2$ treatment as well as m/z 102 and m/z 74 after BiPO_4/UV treatment. Product 1 was identified as thiourea dioxide with m/z 107, whereas product 2 was identified as melamine with m/z 126. Besides, after the treatment of BiPO_4/UV , product 3 was identified as biuret with m/z 102.

Based on the analytical intermediates mentioned above, the transformation pathway of thiourea by the $\text{O}_3/\text{H}_2\text{O}_2 + \text{BiPO}_4/\text{UV}$ synergy technique is illustrated in Fig. 9. The first step of the $\text{O}_3/\text{H}_2\text{O}_2$ treatment mainly contributed to thiourea degradation by hydroxyl radicals together with direct oxidation by hydrogen peroxide and ozone. Thiourea was converted to thiourea dioxide and melamine. We predicted that with further oxidation of hydroxyl radicals, an unstable intermediate was generated and polymerized into melamine immediately.

The mechanism of hydroxyl radicals' oxidation mainly occurred *via* the following two steps: first, the addition to unsaturated carbon; second, hydrogen abstraction from saturated carbon.^{34,35} According to this, hydroxyl radicals were weak in melamine mineralization. However, the treatment of BiPO_4/UV after $\text{O}_3/\text{H}_2\text{O}_2$ not only increased the amount of hydroxyl

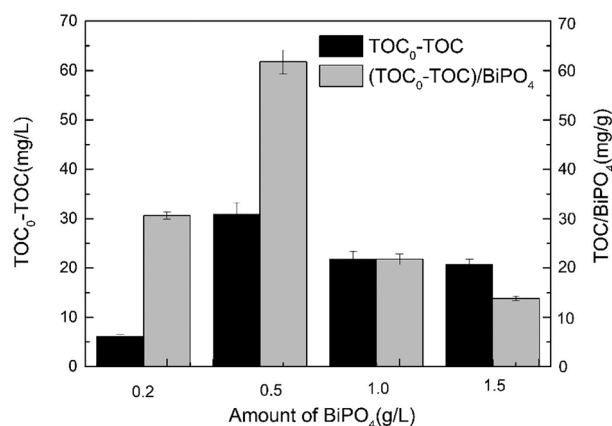


Fig. 8 TOC removal amount and $(\text{TOC}_0 - \text{TOC})/\text{BiPO}_4$ ratio in the post-treatment process. The TOC amount after pre-treatment was 174.5 mg L^{-1} , H_2O_2 residue was 71.45 mg L^{-1} , and UV intensity was 4.73 mW cm^{-2} .



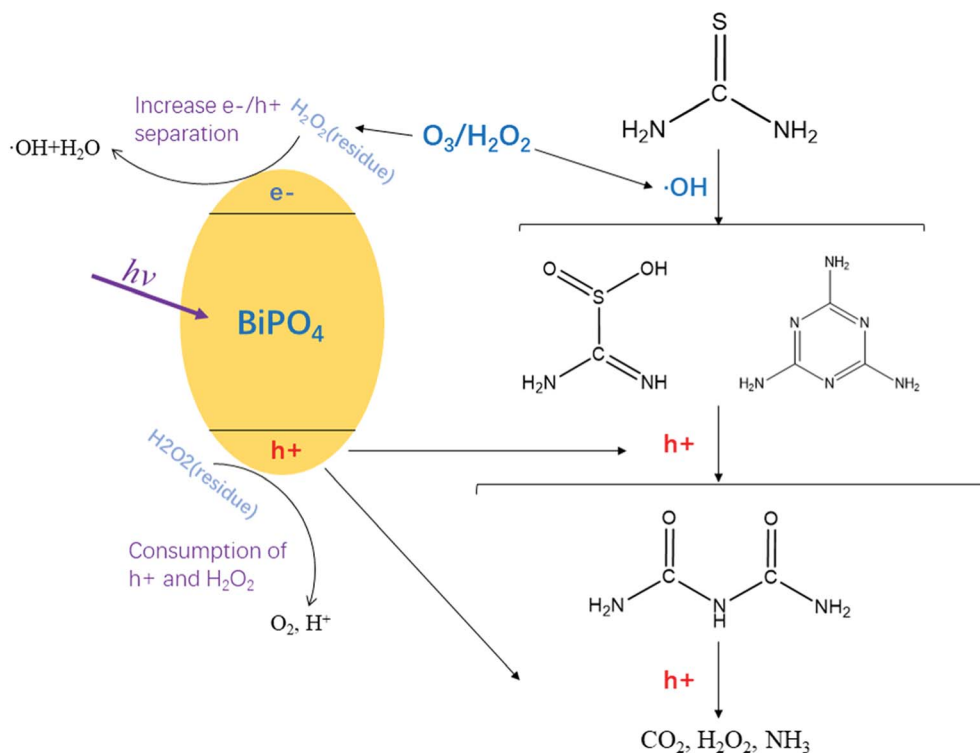


Fig. 9 Prediction of mineralization pathway of thiourea by the $O_3/H_2O_2 + BiPO_4/UV$ synergy technique.

radicals, but also introduced the process of hole mineralization. Thus, after the first step of O_3/H_2O_2 , $BiPO_4/UV$ served as the second step to generate holes that carried out the electron transfer oxidation³⁶ so that melamine and thiourea dioxide can be further transformed into biuret and then mineralized into H_2O and CO_2 . In addition, the H_2O_2 residues from O_3/H_2O_2 not only increased the separation of e^-/h^+ but also induced $\cdot OH$ generation through the reaction between e^- and H_2O_2 ; thus, more $\cdot OH$ species could be generated, which contributed to acceleration of thiourea degradation and mineralization. No thiourea was detected after treatment with the $O_3/H_2O_2 + BiPO_4/UV$ synergy technique, and it was transformed into substances introduced before without biotoxicity, which can be further treated by biological methods in a municipal wastewater treatment plant.

4. Conclusions

TOC removal, H_2O_2 utilization and the transformation pathway of thiourea by the newly invented $O_3/H_2O_2 + BiPO_4/UV$ synergy technique was investigated in this study. Higher mineralization and degradation efficiency of thiourea was attained compared with that of O_3/H_2O_2 and $BiPO_4/UV/H_2O_2$ single-processes and $O_3/H_2O_2 + UV$ process. Thiourea could be completely transformed into substances without biotoxicity. The synergy between H_2O_2 and $BiPO_4$ improved the TOC removal and also the utilization of residual H_2O_2 left from the O_3/H_2O_2 treatment. H_2O_2 captured e^- on $BiPO_4$, which increased the separation of e^- and h^+ and generated more $\cdot OH$ in a shorter period. The amount of added H_2O_2 influenced both O_3/H_2O_2 and $BiPO_4/UV$

steps, especially $BiPO_4/UV$, because the addition of excess H_2O_2 tended to generate more residual H_2O_2 , which influenced the synergy between H_2O_2 and $BiPO_4$ and decreased the amount of TOC removal. Excessive catalyst loading showed a negative effect on the mineralization efficiency. O_3/H_2O_2 mainly degraded thiourea into thiourea dioxide and melamine by $\cdot OH$, and $BiPO_4/UV$ degraded them into biuret and methyl carbamate, followed by their further mineralization into CO_2 and H_2O .

Conflicts of interest

The authors have no conflicts of interest to declare.

Acknowledgements

We greatly acknowledge the financial support from the National Science and Technology Major Projects of Water Pollution Control and Management of China (2014ZX07206001).

References

- 1 P. Manivel, K. Prabakaran, V. Krishnakumar, F. R. N. Khan and T. Maiyalagan, *Ind. Eng. Chem. Res.*, 2014, **25**, 395–402.
- 2 R. S. Upadhayaya, G. M. Kulkarni, N. R. Vasireddy, J. K. Vandavasi, S. S. Dixit, V. Sharma and J. Chattopadhyaya, *Bioorg. Med. Chem.*, 2009, **17**, 4681–4692.
- 3 C. Kannan, P. Aditi and B. Zwanenburg, *Crop Prot.*, 2015, **70**, 92–98.



- 4 G. Vinithra, S. Suganya and S. Velmathi, *Tetrahedron Lett.*, 2013, **54**, 5612–5615.
- 5 L. Zhou, X. Hu and S. Wu, *Surf. Coat. Technol.*, 2013, **228**, S171–S174.
- 6 A. Korhonen, K. Hemminki and H. Vainio, *Basic Clin. Pharmacol. Toxicol.*, 2010, **51**, 38–44.
- 7 G. Mendoza, A. I. Álvarez, M. M. Pulido, A. J. Molina, G. Merino, R. Real, P. Fernandes and J. G. Prieto, *Carbohydr. Res.*, 2007, **342**, 96–102.
- 8 S. Dales and W. S. Hoar, *Can. J. Zool.*, 2011, **32**, 244–251.
- 9 S. A. Khan, N. Singh and K. Saleem, *Eur. J. Med. Chem.*, 2008, **43**, 2272–2277.
- 10 A. Y. Lin, S. C. Panchangam, C. Chang, P. K. A. Hong and H. Hsueh, *J. Hazard. Mater.*, 2012, **243**, 272–277.
- 11 S. Popiel, T. Nalepa, D. Dzierżak, R. Stankiewicz and Z. Witkiewicz, *J. Hazard. Mater.*, 2009, **164**, 1364–1371.
- 12 J. J. Wu, M. Muruganandham and S. H. Chen, *J. Hazard. Mater.*, 2007, **149**, 218–225.
- 13 S. Esplugas, J. Gimenez, S. Contreras, E. Pascual and M. Rodriguez, *Water Res.*, 2002, **36**, 1034–1042.
- 14 H. Zangeneh, A. A. L. Zinatizadeh and M. Feizy, *J. Ind. Eng. Chem.*, 2014, **20**, 1453–1461.
- 15 T. Wu and J. D. Englehardt, *Environ. Sci. Technol.*, 2012, **46**, 2291–2298.
- 16 Y. Lee, D. Gerrity, M. Lee, S. Gamage, A. Pisarenko, R. A. Trenholm, S. Canonica, S. A. Snyder and U. von Gunten, *Environ. Sci. Technol.*, 2016, **50**, 3809–3819.
- 17 J. A. Zazo, J. A. Casas, A. F. Mohedano, M. A. Gilarranz and J. J. Rodríguez, *Environ. Sci. Technol.*, 2005, **39**, 9295–9302.
- 18 C. Pan and Y. Zhu, *Environ. Sci. Technol.*, 2010, **44**, 5570–5574.
- 19 C. Pan and Y. Zhu, *Catal. Sci. Technol.*, 2015, **5**, 371–383.
- 20 Y. Liu, Y. Zhu, J. Xu, X. Bai, R. Zong and Y. Zhu, *Appl. Catal., B*, 2013, **142–143**, 561–567.
- 21 Y. Zhu, Y. Liu, Y. Lu, H. Wang, Q. Ling and Y. Zhu, *Acta Phys.-Chim. Sin.*, 2013, 576–584.
- 22 R. M. Sellers, *Analyst*, 1980, **105**, 950.
- 23 H. Christensen, K. Sehested and H. Corfitzen, *J. Phys. Chem.*, 1982, **86**.
- 24 M. F. Kabir, E. Vaisman, C. H. Langford and A. Kantzas, *Chem. Eng. J.*, 2006, **118**, 207–212.
- 25 M. Tokumura, A. Ohta, H. T. Znad and Y. Kawase, *Water Res.*, 2006, **40**, 3775–3784.
- 26 S. Haji, B. Benstaali and N. Al-Bastaki, *Chem. Eng. J.*, 2011, **168**, 134–139.
- 27 E. S. Elmolla and M. Chaudhuri, *Desalination*, 2010, **252**, 46–52.
- 28 V. Auguliaro, E. Davì, L. Palmisano, M. Schiavello and A. Sclafani, *Appl. Catal.*, 1990, **65**, 101–116.
- 29 C. Chiou, C. Wu and R. Juang, *Chem. Eng. J.*, 2008, **139**, 322–329.
- 30 Y. Zhang, R. Selvaraj, M. Sillanpää, Y. Kim and C. Tai, *Chem. Eng. J.*, 2014, **245**, 117–123.
- 31 S. Lathasree, A. N. Rao, B. SivaSankar, V. Sadasivam and K. Rengaraj, *J. Mol. Catal. A: Chem.*, 2004, **223**, 101–105.
- 32 A. Burns, W. Li, C. Baker and S. I. Shah, *MRS Proceedings*, 2001, 703.
- 33 A. Sobczyński, Ł. Duczmal and W. Zmudziński, *J. Mol. Catal. A: Chem.*, 2004, **213**, 225–230.
- 34 J. A. Khan, X. He, N. S. Shah, H. M. Khan, E. Hapeshi, D. Fatta-Kassinos and D. D. Dionysiou, *Chem. Eng. J.*, 2014, **252**, 393–403.
- 35 T. Olmez-Hanci and I. Arslan-Alaton, *Chem. Eng. J.*, 2013, **224**, 10–16.
- 36 A. Y. Ahmed, T. A. Kandiel, I. Ivanova and D. Bahnemann, *Appl. Surf. Sci.*, 2014, **319**, 44–49.

